



OPEN

ID1 marks the tumorigenesis of pancreatic ductal adenocarcinoma in mouse and human

Yuanxin Tang¹, Sheng Zhang¹, Jiazi Li¹, Chunli Wu² & Qing Fan¹✉

Pancreatic Ductal Adenocarcinoma (PDAC) is a deadly disease that has an increasing death rate but no effective treatment to now. Although biological and immunological hallmarks of PDAC have been frequently reported recently, early detection and the particularly aggressive biological features are the major challenges remaining unclear. In the current study, we retrieved multiple scRNA-seq datasets and illustrated the genetic programs of PDAC development in genetically modified mouse models. Notably, the transcription levels of *Id1* were elevated specifically along with the PDAC development. Pseudotime trajectory analysis revealed that *Id1* was closely correlated with the malignancy of PDAC. The gene expression patterns of human PDAC cells were determined by the comparative analysis of the scRNA-seq data on human PDAC and normal pancreas tissues. *ID1* levels in human PDAC cancer cells were dramatically increased compared to normal epithelial cells. *ID1* deficiency in vitro significantly blunt the invasive tumor-formation related phenotypes. IPA analysis on the differentially expressed genes suggested that EIF2 signaling was the core pathway regulating the development of PDAC. Blocking EIF2 signaling remarkably decreased the expression of *ID1* and attenuated the tumor-formation related phenotypes. These observations confirmed that *ID1* was regulated by EIF2 signaling and was the critical determinant of PDAC development and progression. This study suggests that *ID1* is a potential malignant biomarker of PDAC in both mouse models and human and detecting and targeting *ID1* may be a promising strategy to treat or even rescue PDAC.

Abbreviations

scRNA-seq	Single cell RNA-sequencing
PDAC	Pancreatic ductal adenocarcinoma
ID1	Inhibitor of DNA binding 1
EIF2A	Eukaryotic translation initiation factor 2A
EDU	5-Ethynyl-2'-deoxyuridine
KIC	$Kras^{LSL-G12D/+}Ink4a^{fl/fl}Ptf1a^{Cre/+}$
KPFC	$Kras^{LSL-G12D/+}Trp53^{fl/fl}Pdx1^{Cre/+}$
KPC	$Kras^{LSL-G12D/+}Trp53^{LSL-R172H/+}Ptf1a^{Cre/+}$
KPC2	$Kras^{LSL-G12D/+}Trp53^{LSL-R172H/+}Pdx1^{Cre/+}$
IPA	Ingenuity Pathway Analysis
EMT	Epithelial-mesenchymal transition

Pancreatic Ductal Adenocarcinoma (PDAC), the most prevalent neoplastic disease of the pancreas, constitutes more than 90% of all pancreatic cancers¹ and is the fourth most frequent cause of cancer-related deaths in the past few decades with poor prognosis and low survival rate²⁻⁵. The low survival rate of PDAC is most importantly because of the delayed clinical symptoms at advanced stages when the tumor initiates the invasion into the surrounding structures or metastasizes^{3,4}. The reason of this is most due to the lack of biomarkers of PDAC carcinogenesis, which is making it more urgent to discover novel genetic or biological hallmarks to detect the development of PDAC.

¹Department of General Surgery, The Fourth Affiliated Hospital of China Medical University, Shenyang, China. ²Department of Radiation Oncology, The Fourth Affiliated Hospital of China Medical University, Shenyang, China. ✉email: qingfan@cmu.edu.cn

scRNA-seq has been well established in recently years⁶ and has overcome the limitations of traditional microarray assays and bulk RNA sequencing methods, by sequencing the whole transcriptome at a single-cell resolution and distinguishing different cell types in tumor tissues⁷. scRNA-seq promises a better way for us to understand the tumor microenvironment and intratumor heterogeneity⁸, and enables a clearer understanding of the molecular mechanisms of tumor occurrence, and reveals the somatic mutations all throughout the course of tumor evolution⁹. PDAC is also a kind of solid tumors comprising both tumor cells and also an extremely complex microenvironment with which the tumor cells constantly interact during tumor formation¹⁰. Detailed characterization of the cellular composition of the tumor microenvironment is critical for the understanding of the disease and the potential therapies. To achieve that, a recent study used scRNA-seq technology to agnostically profile cell heterogeneity during different stages of PDAC progression in several well-established genetically engineered mouse models, including early and late KIC, KPfC, KPC and described the landscape of cellular heterogeneity during the progression of PDAC¹¹. Another recent study complemented this cellular landscape by applied scRNA-seq on another PDAC mouse model (termed as KPC2 here)¹². For human pancreas and related malignance study, a scRNA-seq study described the transcriptome of normal adult human pancreatic cell types and identified subpopulations of existing cell types and markers¹³. This open accessed dataset provided a perfect database as the controls of other pancreatic malignant diseases including PDAC. A more specific study targeting pancreatic preinvasive lesions analyzed tumor-associated stromal, immune, endothelial and fibroblast cells and identified signals that might support tumor development by single-cell transcriptome analysis of human PDAC¹⁴.

By recruiting all the above scRNA-seq databases, in the current study we integrated the normal epithelial cells, pre-malignant and malignant cancer cells from both mouse models and human PDAC tissues. We generated a completed genetic program of PDAC development and progression and identified the critical genetic genes that potentially marked the PDAC formation in mouse and human, among which ID1 is the most specific and significant one. The roles of ID1 in PDAC have been studied for decades by several recent studies^{15–17}. The reported mechanisms included mediating cells proliferation, migration and invasion abilities, as well as the expression of HIF-1 α , VEGF and MMP-9^{15,16} escaping from TGF β tumor suppression¹⁷ and epithelial-mesenchymal transition (EMT)¹⁸. All these studies made it convincing that ID1 was significantly involved in PDAC progression. However, most of the studies above were conducted in vitro either on cell lines or by brief histology staining without any well-established validation in vivo and the detailed PDAC progression and potential upstream signaling pathways were not yet clear up to now. The association of ID1 in purified PDAC cancer cells has never been described.

In the current study, by comparative analysis, an elevated transcription of ID1 in PDAC was validated in several independent scRNA-seq and microarray datasets in both mouse and human. More importantly, the transcription levels of ID1 were dramatically increased along with the progression of PDAC. Signaling pathway and upstream regulator analysis revealed that EIF2 signaling was core signaling regulating PDAC progression and ID1 dysregulation, and this regulation genetic axis was consistent with the observations in neuroblastoma¹⁹. Blocking EIF2 signaling remarkably downregulated the expression level of ID1 and blunt the formation of PDAC in vitro, suggesting that ID1 was regulated by EIF2 signaling and achieved its functions in controlling tumorigenesis of PDAC.

Based on these data and in coordinate with previous studies, we assume that ID1 was a promising biomarker for the malignance of PDAC and targeting or monitoring ID1 might serve as a potential method for advanced PDAC diagnosis and therapeutic treatment in precise medicine clinically.

Materials and methods

Cell line. Pancreatic Carcinoma cell lines, HS-766T and PANC-1, were obtained from ATCC and were maintained in DMEM supplied with 10% FBS and the antibiotics Penicillin (100 IU) and Streptomycin (100 μ g/ml).

Gene knockdown assay. HS-766T or PANC-1 cells were split into 6-well plates and cultured until about 50% confluency. Lentivirus particles targeting specific genes (shID1 Lentiviral Particles sc-44267-V and shEIF2A Lentiviral Particles sc-35272-V, Santa Cruz Biotechnology) and the control shRNA Lentiviral particles (sc-108080, Santa Cruz Biotechnology) were pre-mixed with Polybrene (10 μ g/ml) in complete medium. The cells were cultured with Lentiviral Particles (2.0×10^5 IFU/well) for overnight and one well was used as a selecting control. The medium was refreshed the next day. 48 h after Lentiviral Particles infection, the cells were treated with puromycin (5 μ g/ml) for 1 to 2 days until all the cells in the selecting control well were dead. For the EIF2A rescue experiments, recombinant human EIF2A protein (Recombinant Human eIF2 α /EIF2S1 His Protein, NOVUS Biologicals, NBP1-44467) was added into ID1 knockdown HS-766T stable line and the cells were harvested 12 h after treatment for qRT-PCR and 24 h after treatment for western blotting.

qRT-PCR. RNA extraction was performed by RNeasy Kits (QIAGEN, 74004) from the cells after infection according to manufacturer's instructions and RNA concentration and purify were quantified by a NanoDrop™ 2000. Reverse transcription was performed on 40 ng purified RNA by M-MLV Reverse Transcriptase system (Promega, M1701). The relative mRNA expression levels of target genes were determined by PowerUp SYBR Green Master Mix kit (Thermo Fisher Scientific, A25742). Human GAPDH was used as an internal control gene and relative expression levels were calculated by using the $2^{-\Delta\Delta C_t}$ method. The sequences of specific primer pairs are listed below: ID1: forward, 5'-ATTACGTGCTCTGTGGGTCTCC-3', reverse, 5'-TAGTAGGTGTGCAGAGAGGAGC-3'; Human eIF2A qPCR Primer Pair (SinoBiological, HP100187); GAPDH: forward, 5'-ACC CAGAAGACTGTGGATGG-3', reverse, 5'-TTCTAGACGGCAGGTCAGGT-3'.

Western blotting. Total proteins were extracted from the cells by RIPA Lysis and Extraction Buffer (Thermo Fisher Scientific, 89900) with Halt™ Protease and Phosphatase Inhibitor added (Thermo Fisher Scientific, 78440).

Same amounts of total proteins from each sample were loaded into SDS-PAGE gels for separation and were transferred to PVDF membrane. Primary antibodies targeting specific proteins were diluted and added to the membrane and HRP conjugated secondary antibodies were used to visualize the signals. Antibodies used are listed below: rabbit anti-Id1 polyclonal antibody (abcam, ab230679), mouse anti-eIF2A monoclonal antibody (3A7B11) (abcam, ab181467), rabbit anti-GAPDH monoclonal antibody (14C10) (Cell Signaling Technology, 2118), anti-rabbit IgG, HRP-linked antibody (Cell Signaling Technology, 7074), anti-mouse IgG, HRP-linked antibody (Cell Signaling Technology, 7076).

Migration assay. 24-well transwell cell culture chambers (Corning, 353226) were used for migration assays to determine the cell motile capacities. Briefly, 100 thousand cells in 200 μ l serum-free medium were loaded into the chambers and medium with FBS as attractant was added into the bottom wells. After culturing for overnight (24 h), cells were fixed with methanol and stained with Trypan blue for visualization. Cells remaining in the transwell chambers were swiped off with cotton swabs and the cells in the bottom were regarded as migrating cells. Quantifications of the cell migration ratio were conducted by cell counting and normalized to the cell numbers of the control groups.

Soft agar assay. The Soft Agar Assay for Colony Formation is an anchorage independent growth assay in soft agar, which is considered the most stringent assay for detecting malignant transformation of cells. Soft agar assays were performed in 24-well plate coated with 0.6% agarose diluted in DMEM. 10 thousand cells resuspended in DMEM containing 10% FBS and 0.35% agarose were plated and cultured for three weeks under standard cell culture conditions. Each group was triplicated. Cells were fixed with 10% Neutral buffered formalin and stained with 0.005% Crystal Violet for more than 1 h, and the colonies were imaged and counted by a light microscopy.

EDU proliferation assay. Proliferation rates of cells at different condition were performed by EdU Alexa Fluor™ 488 Imaging Kit (Thermo Fisher Scientific, C10337) according to manufacturer's instructions. In brief, a 2 \times working solution of EdU was prepared in complete medium and added into cell culture. After 4-h culturing, the medium was discarded, and the cells were immediately proceeded to cell fixation and permeabilization with a Fixation/Permeabilization solution (Thermo Fisher Scientific, eBioscience™ Foxp3/Transcription Factor Staining Buffer Set 00-5523-00). The reaction cocktail was prepared and added to each well and the cell plate was rocked briefly to ensure that the reaction cocktail was distributed evenly. After incubation for 30 min at room temperature protecting from light, the cocktail was washed off and the cells were analyzed by a BD Arial II cell analyzer.

Cell apoptosis assay. Cell apoptosis of ID1 knockdown and control HS-766T cells were determined by Annexin V apoptosis detection kit (STEMCELL Technologies Scientific, 100-0338) according to manufacturer's instructions. In brief, cell medium was aspirated, and the cells were washed with PBS for twice. The trypsinized cells were resuspended at a concentration of 1.0×10^6 cells/ml in Annexin V Binding Buffer and Annexin V and 7-AAD were added at 5 μ l/100 μ l. The cells were incubated with Annexin V and 7-AAD at room temperature protecting from light for 15 min and washed with Binding Buffer for analysis by flow cytometry. For the flow cytometry analysis, cell populations were divided into four quadrants (Q1–Q4) with percentage quantified and populations in Q2 and Q3 were regarded as late apoptotic cells.

scRNA-seq and microarray data accession. Open accessed scRNA-seq data and microarray data used in this study were retrieved from the NCBI Gene Expression Omnibus²⁰ and the corresponding raw data from NCBI Sequence Read Archive (SRA). The accession numbers of the data on mouse PDAC mouse models, normal pancreas, early KIC, late KIC, late KPFC and late KPC, were GSE125588 and PRJNA516878. Data from another mouse PDAC model, late KPC2, were from GSE129455 and PRJNA531464. ScRNA-seq data on normal pancreas and PDAC were retrieved from GSE85241 and PRJNA337935, GSE141017 and PRJNA604712 respectively. Microarray data on human PDAC and matched control samples were from GSE16515, GSE28735, GSE32676 and GSE15471.

Bioinformatic analysis. Bioinformatic analysis on scRNA-seq data were performed under the guidance of standard tutorial in R/R-studio. Briefly, low quality cells were removed, and the cell clusters were identified based on gene (feature) transcripts. Differential gene expression was performed to define the cell types and specific gene of each cluster and each cell type. Data integration was done when multiple datasets were needed for analysis and comparison. Ingenuity Pathway Analysis (IPA) was used to demonstrate the Canonical Signaling Pathways, Upstream Regulators and Graphic Networks of specific cell clusters based on the top differentially expressed genes. Slingshot packages were used to do the pseudotime analysis. Microarray data were also analyzed in R/R-studio after data normalization and gene ID and symbol annotation.

Statistical analysis. All statistical data were analyzed and visualized by GraphPad Prism 8 software. Student's two-tailed t test was used for comparing difference significance between 2 groups and a p value $pf < 0.05$ was considered statistically significant. Each experiment was repeated for at least three times and all results were presented as mean \pm SEM.

Results

Access of the scRNA-seq data on PDAC mouse models. As the development of single cell omics technologies, many of recent studies have focused more on the development and heterogeneities of malignant diseases, especially in mammary tumors. To profile cell populations and understand the phenotypic changes during PDAC progression, a recent study used scRNA-seq to agnostically profile cell heterogeneity during different stages of PDAC progression in genetically engineered mouse models¹¹, including normal and four PDAC models, early KIC, late KIC²¹, late KPfC²² and late KPC²³. Violin plots were used to visualize the cells qualities and the low-quality cells or doublets were removed (Supplementary Fig. S1A,B). Batch effects were corrected and retained cells were clustered and visualized by UMAP (Supplementary Fig. S2A,B). Cell types were identified by checking canonical cell type specific markers (Supplementary Fig. S2C,D)¹⁴. Batch correction was confirmed by split UMAPs (Supplementary Fig. S3A), and cell-type identification was confirmed by the expression of the cell type markers visualized by violin plots (Supplementary Fig. S3B). Gene expression patterns were specified by heatmap of top 100 genes of each defined cell type (Supplementary Fig. S2E). We then subset and clustered the epithelial lineage cells and identified the normal acinar (Amy1+ and Amy2a2+) and islet/ductal cells (Pyy+ and Sst+, Ins1+ and Ins2+) as well as a cancer cell cluster with normal epithelial lineage marker expression excluded (Sox9+ and Krt18+) (Fig. 1A–C). All the cells in cancer cluster were contributed by the PDAC cancer models (Fig. 1A). We also performed the differential expression (DE) analysis on the epithelial cell lineages among the different models and found the DE genes between normal and PDAC models (Fig. 1D). To demonstrate the genetic programs associated with the development of PDAC, we identified the genes dysregulated in the PDAC models and visualized the top genes by violin plots (Fig. 1E). Several transcriptional factor genes, including Fosb²⁴, Junb²⁵ and Sox4^{26,27} were reported to be associated with development, survival or outcome of pancreatic cancer in human. Among these top transcriptional factor genes, the most correlated gene was Id1, expression of which increased along with development of PDAC with rare transcription in normal and less malignant epithelial cells (Fig. 1E). Besides these transcriptional factor genes, multiple cell surface genes, Keratin and Kruppel Like Factor genes as well as several long intervening noncoding RNAs (LincRNA) were also upregulated in the PDAC models (Fig. 1E). These genes were also commonly reported to be correlated with tumor development²⁸, grading²⁹, suppression^{30,31}, prognosis³², tumorigenicity³³ and risk³⁴ of pancreatic cancer. LincRNA Malat1 promotes aggressive pancreatic cancer proliferation and metastasis via multiple reported signaling pathways^{35–37}. Another LincRNA, Meg3, was commonly reported to be a tumor suppressor gene³⁸ and was also dramatically associated with PDAC development³⁹ and malignance^{40,41}.

By the similar way, we retrieved one more scRNA-seq dataset on another mouse model of late KPC (late KPC2)¹². Cells were clustered (Supplementary Fig. S4C) after quality control (Supplementary Fig. S4A,B) and cell types were defined based on the cell type specific maker gene expression (Supplementary Fig. S4D–F). The epithelial cell lineages (Epi_lin) were extracted and integrated with the Epi_lin extracted above (Fig. 2A). Based on the gene transcriptional patterns of the integrated data (Supplementary Fig. S5A,B), two normal epithelial cell clusters, acinar cell cluster and islet/ductal cell cluster, and two malignant cell clusters were identified (Fig. 2B). The normal epithelial cells were mostly contributed by the normal pancreases tissue and early KIC (Fig. 2C). To confirm that, we quantified the cell percentage of each cell cluster in each mouse model (Fig. 2D). Acinar cell percentage was decreased while percentage of cancer cell Cluster 2 was dramatically increased with the progression of PDAC. Cancer cell Cluster 1 showed highest percentage in early KIC only, suggesting that cluster 1 cancer cells potentially marked the initiation of PDAC in these mouse models. We also validated the transcription of these dysregulated transcriptional factor genes, cell surface protein genes, Kruppel Like Factor genes and LincRNA genes in these PDAC mouse models (Fig. 2E) and many other top genes (Supplementary Fig. S6). These genes showed increased expression in the PDAC models, and the most notable gene was Id1, which showed visible transcription only in late malignant PDAC models by violin plots (Fig. 2E).

Id1 marks the development of PDAC in mouse models. Significant increase in Id1 transcription in mouse models implied that Id1 might be involved in the tumorigenesis of PDAC. To further confirm that, we quantified the percentage of the epithelial/cancer cells with Id1 transcription at Id1 > 1 and found a gradual increased percentage along with the progression of PDAC (Fig. 3A).

To demonstrate the profile differences of two cancer cell clusters identified above, these cells were subset (Fig. 3C), and surprisingly, Id1 transcription in these cancer cells was also significantly associated with the progression of PDAC (Fig. 3B). Again, cancer cells in Cluster 1 were confirmed to be contributed by normal pancreases and early KIC, while Cluster 2 by the other more malignant models (Fig. 3E). Distinct DE patterns of two cancer cell clusters were visualized by heatmap on top 500 genes (Fig. 3D). These patterns were visualized by violin plots of top genes of each cancer cluster, including transcriptional factor genes, Claudin genes, Pancreatic lipase related genes and RNA/RNA-binding genes in Cluster 1, as well as including transcriptional factor genes, Kruppel Like Factor genes, Keratin genes and Epithelial-mesenchymal transition (EMT) related genes in Cluster 2 (Fig. 3F). Notably, many of the specific genes in Cluster 1 were associated with normal development and functions of pancreas epithelial cells^{42–47}. In Cluster 2 the EMT related genes, including Fn1, Vim and Sdc1, were significantly upregulated, suggesting that Cluster 2 underwent active EMT, one of the major features of cancer progression. The transcriptional genes, Kruppel Like Factor genes and Keratin genes, as mentioned above, were closely correlated with tumor development, prognosis and grading of pancreatic cancer (Fig. 3F). More interestingly, Id1 gene was also found to be remarkably upregulated in Cluster 2, suggesting that Id1 was a consistent marker for PDAC progression and malignant cancer cells in mouse models.

Id1 marks differentiation potentials of cancer cell clusters. As two cancer cell clusters were identified, and Cluster 1 showed more normal epithelial cell features, while Cluster 2 demonstrated more malignant

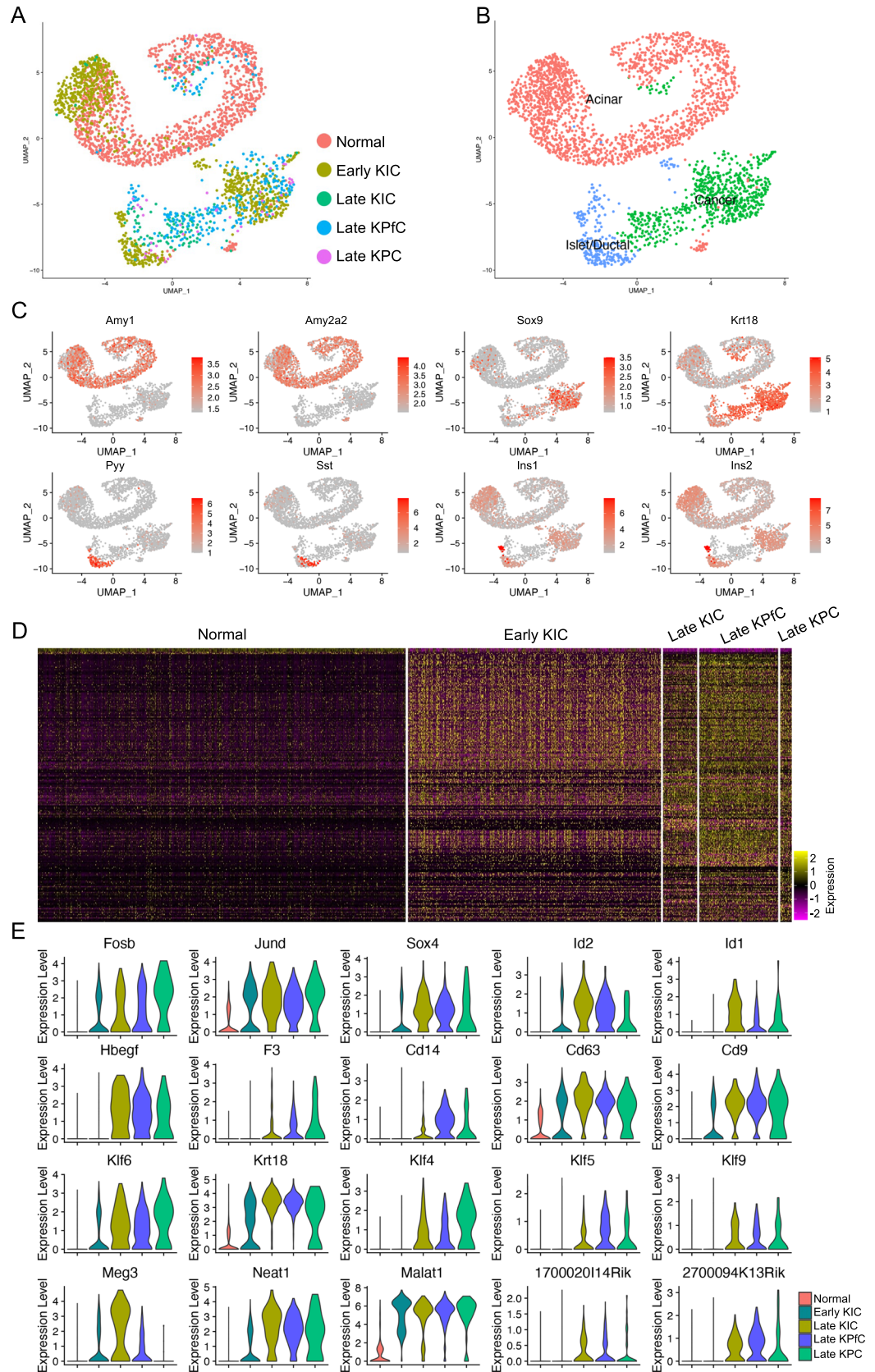


Figure 1. Identification of differentially expressed genes involved in the progression of PDAC development. **(A)** Cell origins of the epithelial/cancer cells from different mouse models. **(B)** Cell type identification of the integrated epithelial/cancer cells. **(C)** UMAP visualization of the expression of canonical epithelial and cancer formation related marker genes. **(D)** Heatmap of the top 100 genes of the epithelial/cancer cells of each mouse model. **(E)** Transcription levels of top five transcription factor, cell surface protein, kruppel like factor and LincRNA genes that were correlated with PDAC progression in mouse models.

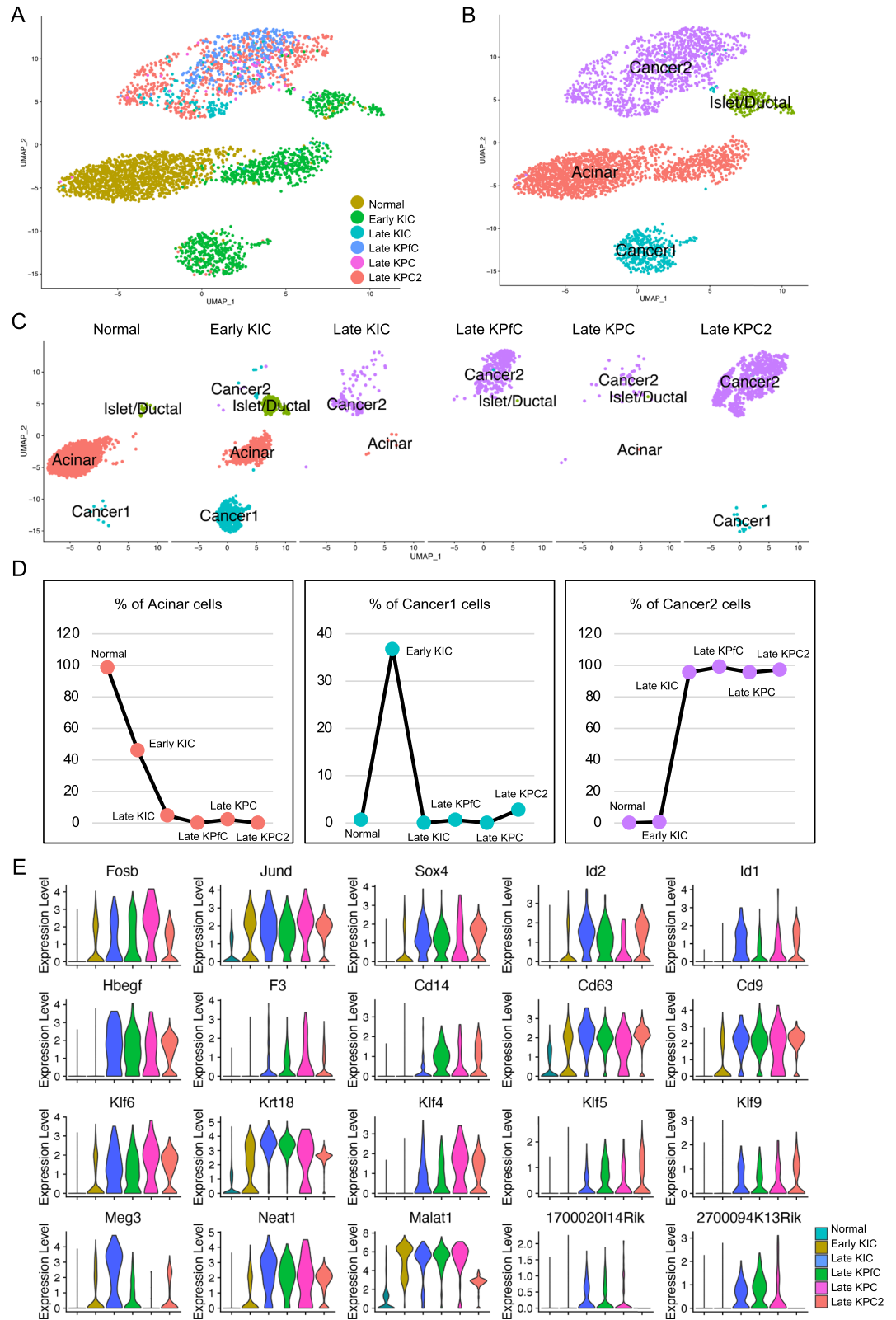


Figure 2. Validation of differentially expressed genes involved in the progression of PDAC development in another model. **(A,B)** Integration of the epithelial/cancer cells from six mouse models **(A)** and cell type definition of the integrated epithelial/cancer cells **(B)**. **(C)** Cell distribution of each cell type in each mouse model. **(D)** Cell percentage of normal epithelial cell and cancer cell clusters in each mouse model. **(E)** RNA levels of the top genes correlated with PDAC progression in the six mouse models.

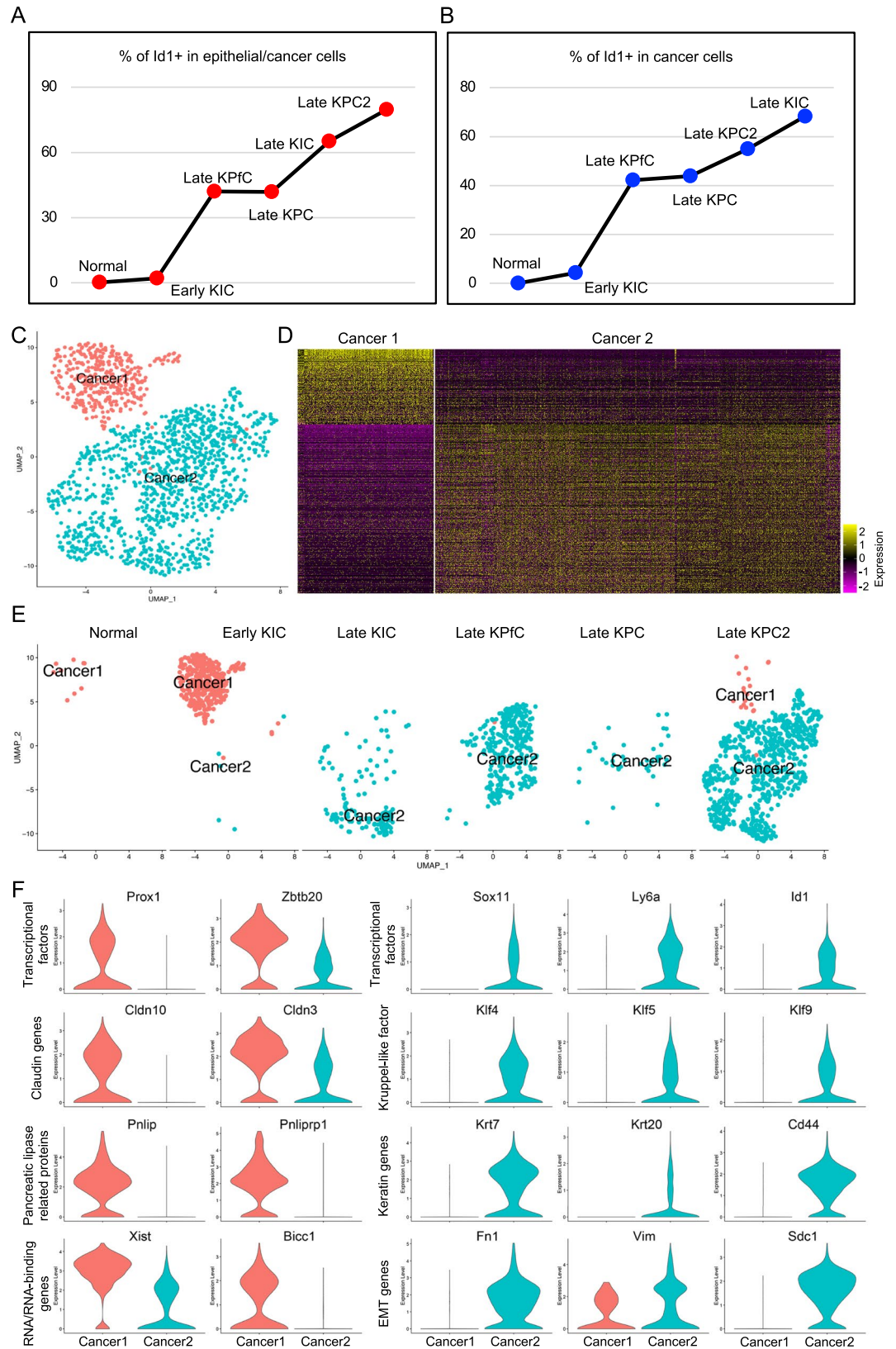


Figure 3. Cancer cell subtypes and corresponding marker genes involved in the progression of mouse PDAC. (A,B) Percentage of Id1+ cells in total epithelial/cancer cells (A) and cancer cells clusters in each mouse model (B). (C) Extraction and re-clustering of the cancer cells. (D) Heatmap of top 500 genes of each cancer cell subpopulation. (E) Cell distribution of each cancer cell subpopulation in each mouse model. (F) Violin plot visualization of the representative top genes of each cancer cell subpopulation.

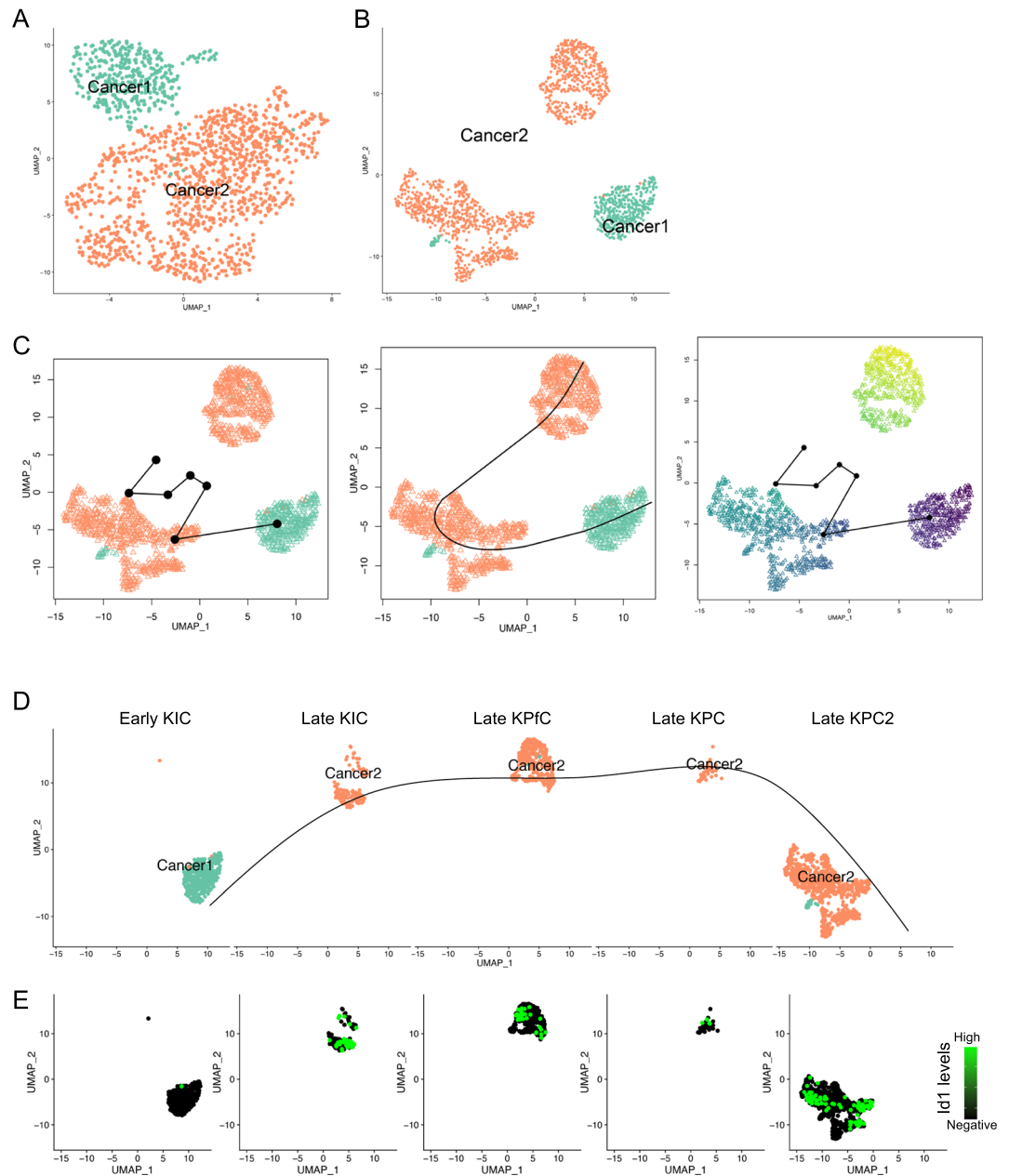


Figure 4. Diversity and differential potentials of the cancer cell subpopulations. (A,B) Cancer cell subcluster distribution (A) and reclustering in Slingshot (B). (C) Trajectory analysis of cancer cells revealed the differentiation direction of the cancer cell subclusters. (D) Distribution of cancer cells from each mouse model in the principal curves. (E) The increase of Id1 transcription was consistent with the differentiation potential of the cancer cell subclusters.

features, we assumed that Cluster 1 was derived from normal epithelial cells and gave rise to Cluster 2. To confirm that, we applied Slingshot packages⁴⁰ to determine the differentiation potentials of the cancer cell clusters. The cancer cells were loaded and visualized in Slingshot (Fig. 4A) and re-clustered, and Cluster 2 were divided into two major subclusters (Fig. 4B). The trajectory analysis revealed that the differentiation was started from Cluster 1 to one subcluster of Cluster 2 and finalized at the other subcluster of Cluster 2 (Fig. 4C). Principal curve in split UMAP also confirmed that the differentiation was initiated from Cluster 1 and finalized at Cluster 2 (Fig. 4D). Surprisingly, Id1 transcription levels were increased with the principal curve of the differentiation potential (Fig. 4E), further suggesting that Id1 was critical for the progression of the cancer. The transcription of the other signature genes of Cluster 1 and Cluster 2 was also illustrated by UMAPs (Supplementary Fig. S7A,B).

To evaluate the different regulation potentials of the two cancer cell clusters, we input the upregulated genes of both Cluster 1 and Cluster 2 into Ingenuity Pathway Analysis (IPA). The top canonical pathways of Cluster 1 included pancreatic cancer initiation pathways, including SPINK1 Pancreatic Cancer Pathway⁴⁸, and multiple

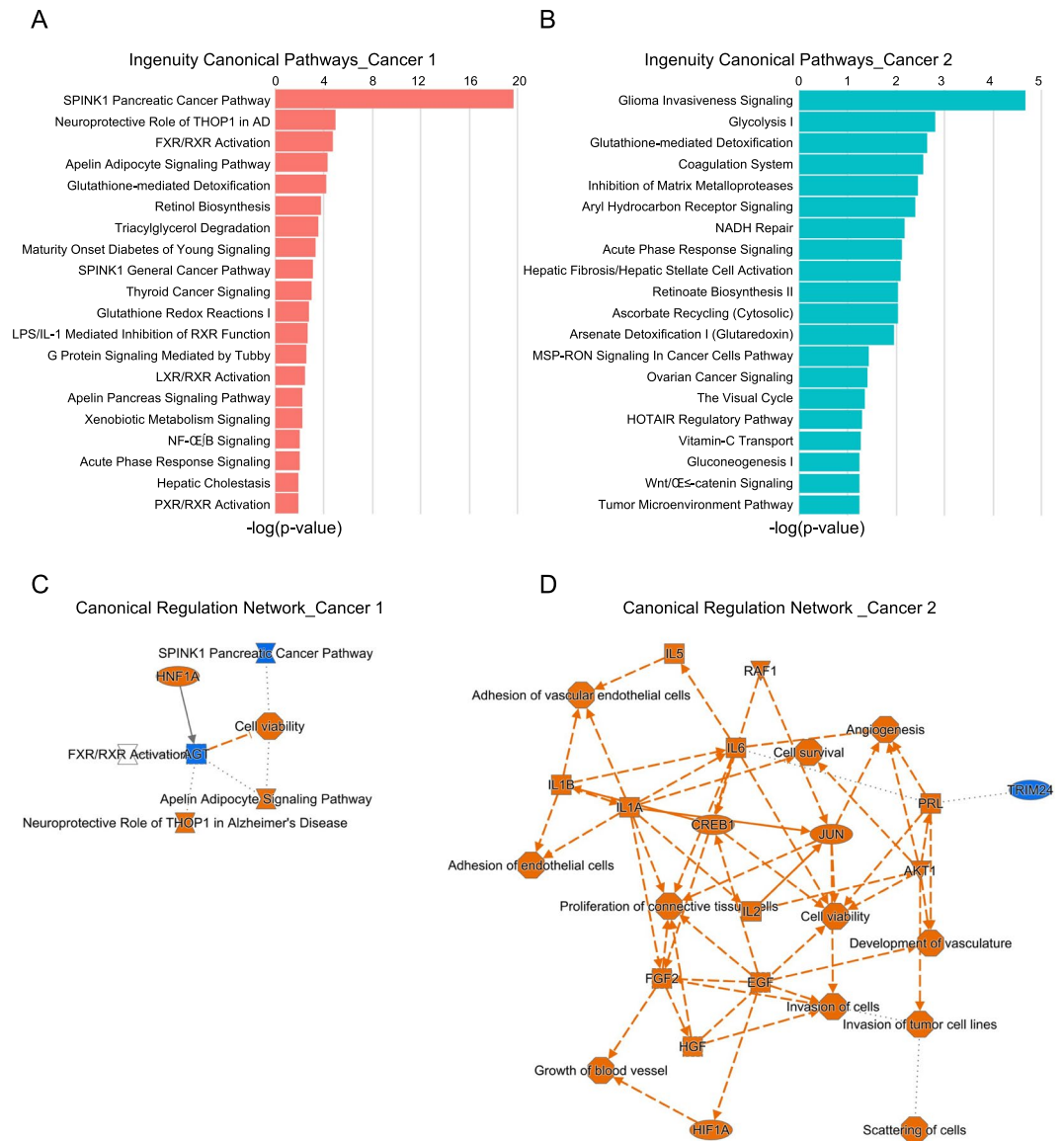


Figure 5. Ingenuity canonical pathways and related pathway networks of the cancer subclusters. (**A,B**) Top 20 ingenuity canonical pathways of cancer cell subcluster 1 (**A**) and cancer cell subcluster 2 (**B**) determined by IPA analysis. (**C,D**) Canonical regulation networks of cancer cell subcluster 1 (**C**) and cancer cell subcluster 2 (**D**) based on ingenuity canonical pathways and upstream regulators by IPA analysis.

normal pancreatic function related pathways (Fig. 5A,C), including FXR/RXR Activation^{49,50}, Apelin Adipocyte Signaling Pathway^{51,52} and Retinol Biosynthesis^{53,54}. Multiple malignant cancer related canonical pathways and upstream regulators were with Cluster 2, including Glioma Invasiveness Signaling, Ovarian Cancer Signaling, Tumor Microenvironment Pathway Invasion of tumor cell lines and Cell survival signaling pathways (Fig. 5B,D). The top upstream regulators of these two clusters were also listed (Supplementary Fig. S7C,D).

Upregulation of ID1 in human PDAC cancer cells. As Id1 gene was significantly upregulated and marked the progression of PDAC in mouse models, to validate this in human, we first accessed a recently published scRNA-seq dataset on normal human pancreas¹³. After quality control (Supplementary Fig. S8A,B), we clustered the cells and defined the major cell types based on canonical cell type marker gene expression (Supplementary Fig. S8C–E). The epithelial cells were the subset and clustered for further analysis (Supplementary Fig. S8F). Similarly, another published scRNA-seq dataset on primary human PDAC was retrieved and quality controlled (Supplementary Fig. S9A,B). Cancer cells were extracted and clustered (Supplementary Fig. S9F) after cell type definition (Supplementary Fig. S9C–E).

Extracted normal epithelial cells and cancer cells were then integrated (Fig. 6A), and DE analysis were performed and visualized by heatmap of top 500 genes to determine the gene expression patterns of each cell condition (Fig. 6B). Notably, the expression levels of normal pancreatic epithelial cell markers, SST and INS,

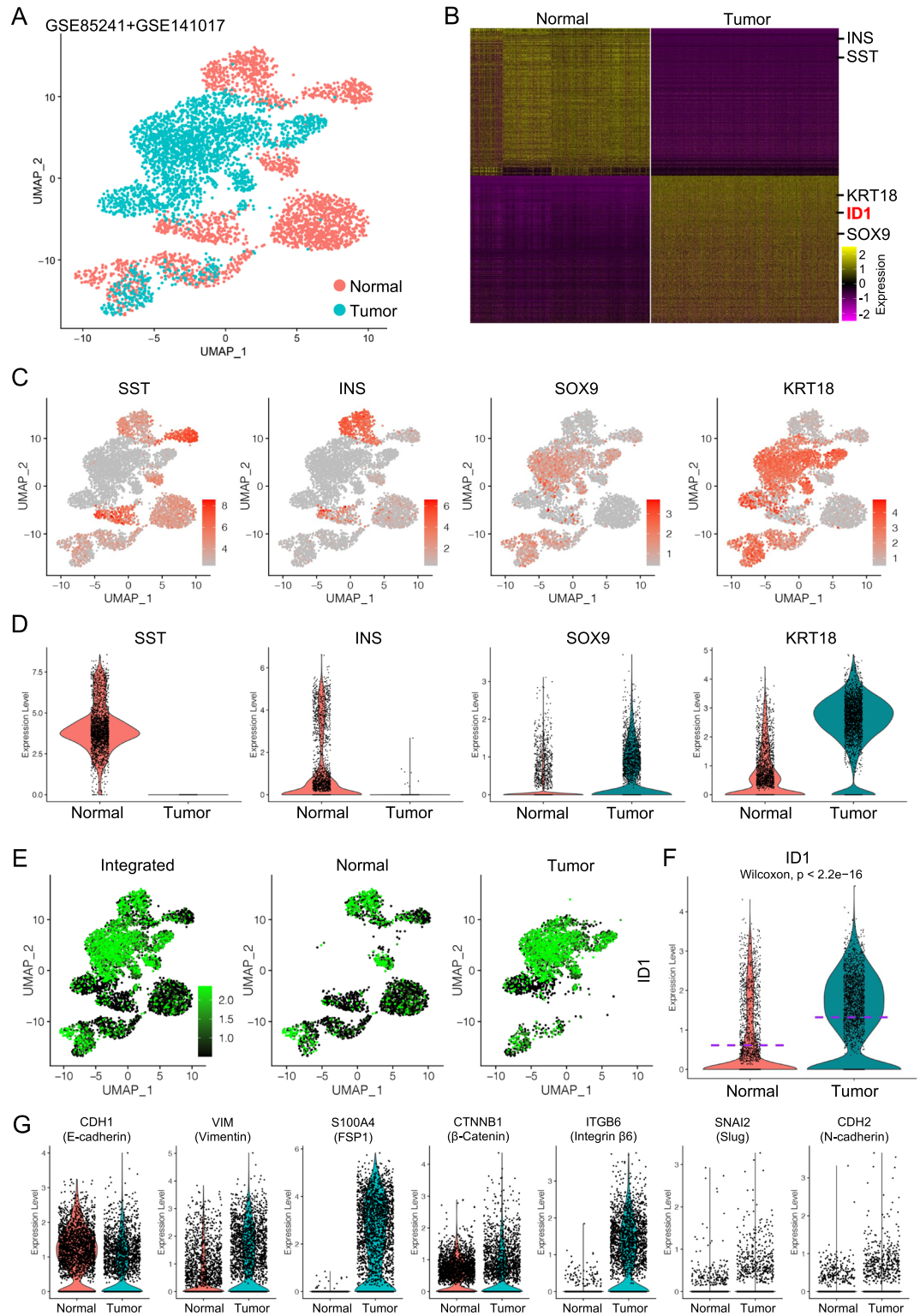


Figure 6. Upregulation of ID1 in human PDAC tumor cells. (A) Integration of the normal human pancreatic epithelial and PDAC cancer cells. (B) Heatmap of top 500 genes of normal human pancreatic epithelial cells and PDAC cancer cells. (C,D) UMAP (C) and violin plot (D) visualization of the expression of normal pancreatic epithelial marker genes and cancer related epithelial marker genes. (E) UMAP visualization of ID1 expression in integrated data and split normal epithelial cells and PDAC cancer cells. (F) Violin plot comparison of ID1 transcription in normal epithelial cells and PDAC cancer cells. (G) Violin plot visualization of EMT related gene expression in normal epithelial cells and PDAC cancer cells.

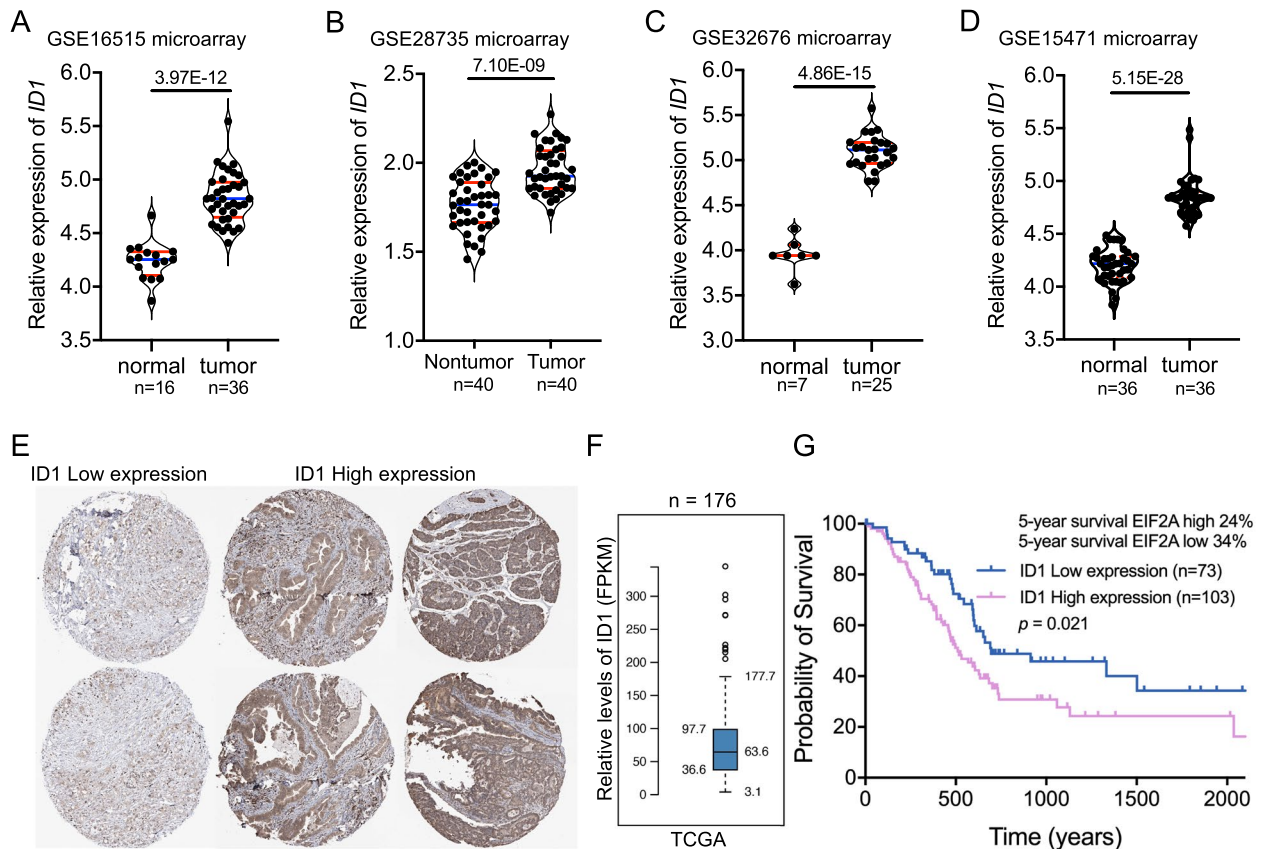


Figure 7. ID1 was upregulated in PDAC tumor tissues and was associated with poor survival of PDAC. (A–D) Comparison of ID1 expression in multiple microarray data of PDAC tumor tissues and matched non-tumor tissues. (E) Differential expression of ID1 in different PDAC patients. Relative expression of ID1 (FPKM) (F) and survival probability of patients with different ID1 expression (G) in TCGA dataset.

were specifically higher compared to cancer cells, suggesting the normal functions of these cells, while malignant marker genes, SOX9 and KRT18, were remarkably upregulated in cancer cells (Fig. 6B–D). More surprisingly, ID1 was the top one transcriptional factor gene (Fig. 6B) and was dramatically upregulated and specific in cancer cells (Fig. 6E,F), suggesting that ID1 might be critical for the PDAC development in human. Also, the activated EMT features were also identified in the PDAC cancer cells, as shown by reduced epithelial marker genes expression and upregulated mesenchymal and EMT marker gene expression (Fig. 6G), suggesting a potential role of ID1 in EMT of PDAC cancer cells in human.

To further confirm the elevated levels of ID1 in PDAC, we accessed multiple microarray datasets based on human PDAC and matched normal tissues. Consistent to the data in scRNA-seq data, in all the microarray datasets ID1 was significantly upregulated in PDAC tumors compared to matched nontumor tissues (Fig. 7A–D). In the TCGA (The Cancer Genome Atlas Program) dataset, tumor tissues from different PDAC patients showed different ID1 expression levels (Fig. 7E,F), and patients with high ID1 expression had significant lower overall survival years compared to those with lower ID1 expression (Fig. 7G). Based on these data, we assumed that ID1 was the key transcriptional factor gene which was closely involved in the tumorigenesis of PDAC in human.

ID1 deficiency reduced PDAC tumor progression in vitro. To confirm the functions of ID1 in PDAC progression, ID1 knockdown assay was conducted on HS-766T cells, a commonly used human pancreatic carcinoma cell line. qRT-PCR and western blotting confirmed the knockdown efficiency at RNA levels (Fig. 8A) and protein levels (Fig. 8B,C). The flow cytometry-based EDU labeling assay was used to determine the cell proliferation rate of the HS-766T cells⁵⁵. ID1 knockdown significantly decreased HS-766T cell proliferation (Fig. 8D,E) and quantified percentage of the EDU+ cells further confirmed that (Fig. 8F). ID1 knockdown also increased HS-766T cell apoptosis determined by Annexin V assay (Fig. 8G,H). In vitro cell migration is a commonly used assay to evaluate cancer cell motility and malignance⁵⁶. We found that ID1 knockdown caused significant decrease in HS-766T cell migration (Fig. 8I,J). The soft agar colony formation assay is a well-established method for characterizing the carcinogenesis capability in vitro and is one of the most stringent tests for malignant transformation in cells⁵⁷. ID1 deficiency significantly reduced the colony formation capacities of HS-766T cells (Fig. 8K,L), suggesting that ID1 was required for the carcinogenesis of the normal pancreatic epithelial cell. The functions of ID1 in PDAC progression were also verified in another PDAC cell line, PANC-1, by cell proliferation, migration and colony formation assays (Supplementary Fig. S10A–H).

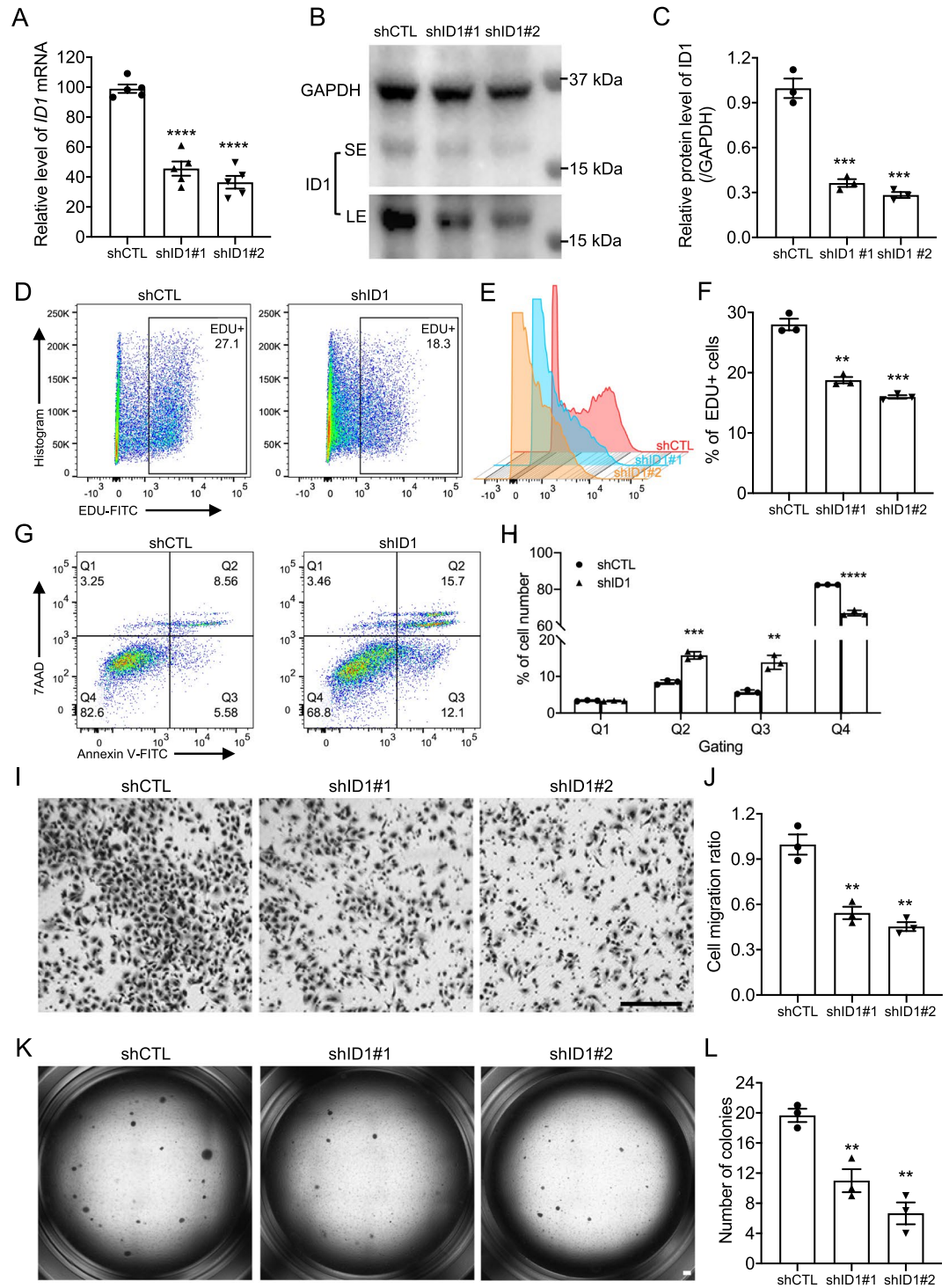


Figure 8. ID1 deficiency attenuated tumor formation related phenotypes. (A) qRT-PCR of the mRNA levels of *ID1* gene in HS-766T cells after knockdown assays (n = 5). (B,C) Western blotting (B) and matched quantification (C) confirmed the efficiency of the knockdown assays (n = 3). (D,E) Flow cytometry analysis of EDU labeled cell proliferation assay in HS-766T cells after knockdown assays. (F) Percentage quantification of the EDU+ proliferating cells after *ID1* knockdown in HS-766T cells (n = 3). (G,H) Cell apoptosis of HS-766T cells after *ID1* knockdown (G) and cell percentage of each gated cell population (H), (n = 3). (I,J) Cell migration (I) and the migration ratio (J) of HS-766T cells after *ID1* knockdown (n = 3). (K,L) Soft agar assays (K) and colony number quantification (L) of HS-766T cells after *ID1* knockdown (n = 3). Three independent repeats or more were performed for each experiment. SE short exposure, LE long exposure. Scale bar, 50 μ m. **p < 0.01; ***p < 0.001, ****p < 0.0001.

EIF2 signaling was the core pathway to regulate ID1 in of PDAC. To determine the upstream regulators and related canonical signaling pathway involved in the ID1 dysregulation and tumor formation, we applied IPA analysis on the DE genes of PDAC cancer cells from the scRNA-seq analysis. Many top canonical pathways and upstream regulators were closely associated with pancreatic cancer (Fig. 9A,B) and the core and the most significant ingenuity canonical pathway was EIF2 signaling (Fig. 9A,B).

As EIF2A is the major component of EIF2 signaling, we verified the expression of EIF2A gene in TCGA dataset and found significant association of EIF2A expression levels with poor survival of PDAC patients (Fig. 9C). These data suggested a core role of EIF2A in determining the malignancy of PDAC. To confirm that, we performed *EIF2A* knockdown assay on HS-766T cells. *EIF2A* knockdown led to a significant decrease in mRNA and protein levels of EIF2A and ID1 (Fig. 9D–F). In addition, adding EIF2A protein to the HS-766T cells significantly induced the elevation of ID1 in HS-766T cells, further validating that ID1 gene was regulated by EIF2 signaling in PDAC cancer cells (Fig. 9G,H). As expected, *EIF2A* knockdown remarkably reduced HS-766T cell proliferation confirmed by flow cytometry-based EDU labeling assay (Fig. 9I–K) and decreased cell motility capacity determined by migration assay (Fig. 9L,M). Also, the colony formation efficiency of HS-766T cells was significantly decreased after *EIF2A* knockdown (Fig. 9N,O), suggesting a decreased ability of transformed cells to grow independently of a solid surface and reduced hallmark of carcinogenesis of these cells. All these data suggested a core regulation potential of EIF2A in tumor formation gene expression patterns and tumorigenesis of PDAC.

Discussion

Pancreatic ductal adenocarcinoma (PDAC), a pancreatic cancer accounts for more than 90% of all pancreatic malignancies, is a devastating malignancy with extremely poor diagnosis and prognosis, as shown by 5-year survival rate of around 5–7% and 1-year survival rate of less than 20% of total cases of all stages^{58–60}. The incidence of PDAC is expected to rise further in the future, and the death rates continued to increase⁵. The low survival rates of PDAC patients are principal since the fact arises that PDAC tumors progress rapidly with very few specific symptoms and are thus usually diagnosed at advanced stages for most patients, as well as aggressive nature of the tumor, and the resistance to chemotherapy and radiotherapy^{61,62}. As a result, there is an urgent need to develop accurate markers of pre-invasive pancreatic neoplasms so as to facilitate prediction of cancer risk and to help diagnose the disease at an earlier stage⁶³. However, although many studies and clinical trials have sought to identify inexpensive, noninvasive, or minimally invasive biomarkers with high sensitivity and specificity for PDAC to improve early diagnosis and subsequent treatment⁶⁴, screening for early diagnosis of PDAC remains challenging and identifying a highly accurate, low-cost screening patient-acceptable test for early PDAC for use in clinical practice remains an important unmet need^{58,63}.

In the current study, by combining multiple datasets, we comprehensively identified that ID1 is a promising pre-malignant biomarker for the screening and monitoring of PDAC development progression. ID1 is a helix-loop-helix (HLH) protein that can form heterodimers with members of the basic HLH family of transcription factors⁶⁵, the overexpression of which has been reported in many types of cancers in either transcriptional or translational levels, including breast, prostate and pancreatic cancers^{66–68}. Several studies have also reported that ID1 has potential to be a prognosis factor associated with patients' survival for PDAC^{16,69}. A histology study from several years ago revealed that ID1 overexpression was significantly related with tumor angiogenesis, higher density of intratumoral vessel, but not associated with a poorer prognosis or a higher proliferative potential in human pancreatic cancers⁶⁹. However ten years later, another study determined that overexpression of ID1 was found to be closely correlated with that of VEGF, an endothelial growth factor that has a central role in cancer angiogenesis^{70,71}, and to be associated with high microvessel density and patient survival in PDAC¹⁶. These studies shared most in common but had a few inconsistent findings. A most recent study has applied 2-Methoxyestradiol (2-ME), a natural derivative of estradiol with ability of suppressing ID1 levels in cell culture, in the function study of ID1 in pancreatic cancer development and progression in vitro¹⁵. Elevated cell proliferation, migration, invasion and tumor xenograft growth caused by ID1 overexpression were blunt by 2-ME treatment in pancreatic cancer cell line¹⁵. TGF β signaling mediates tumor-suppressive or tumor-progressive effects⁷² and causes apoptosis in premalignant cells^{73,74}. Cancer cells derived from PDAC tumor tissues that displayed an active TGF β pathway averted cell apoptosis by transcriptional dysregulation of ID1, also known as an inhibitor of progenitor cell differentiation⁷⁵. Transcriptional induction of ID1 uncoupled TGF β -induced Epithelial-mesenchymal transition (EMT) from apoptosis. The dysregulation of ID1 expression resulted from a diverse set of alterations, including PI3K–AKT signaling pathway mutations¹⁷. These findings shed light on the crucial roles of ID1 in the development of pancreatic cancers and the data were impressive and informative, however many of them were either just bulk histological views on the autopsy slides or plastic phenotypes of cell lines without proper in vivo validation. In this current study, by retrieving multiple scRNA-seq datasets on both mouse models and human PDAC tissues, we purified the epithelial cell lineages and cancer cells and revealed the gene programs of cancer cells at different stages of PDAC progression. Consistently in both mouse and human, ID1 showed a dramatically increased transcription with the progression of PDAC, which was further confirmed by multiple microarray datasets on PDAC and matched non-tumor tissues.

Besides these pancreatic cancer specific findings, ID1 was also found to showed critical roles in Epithelial–Mesenchymal transition (EMT)^{76,77}, one of the critical features of the tumorigenic process⁷⁸. As identified in other cancers, ID1 transcription levels in the cancer cells of both mouse models and human PDAC tissues were closely correlated with cancer cell EMT procession, as well as other tumor-formation related cell phenotypes, including cell proliferation, migration, and colony formation in vitro. Signaling pathway analysis revealed that the functions of ID1 dysregulation in tumor progression were mainly mediated by EIF2 signaling, which was commonly reported as a promising target in cancer therapy⁷⁹. EIF2 signaling activities were reported to be elevated in PDAC tumors, as shown by higher phosphorylated EIF2A, p-EIF2A, expression in PDAC tissues

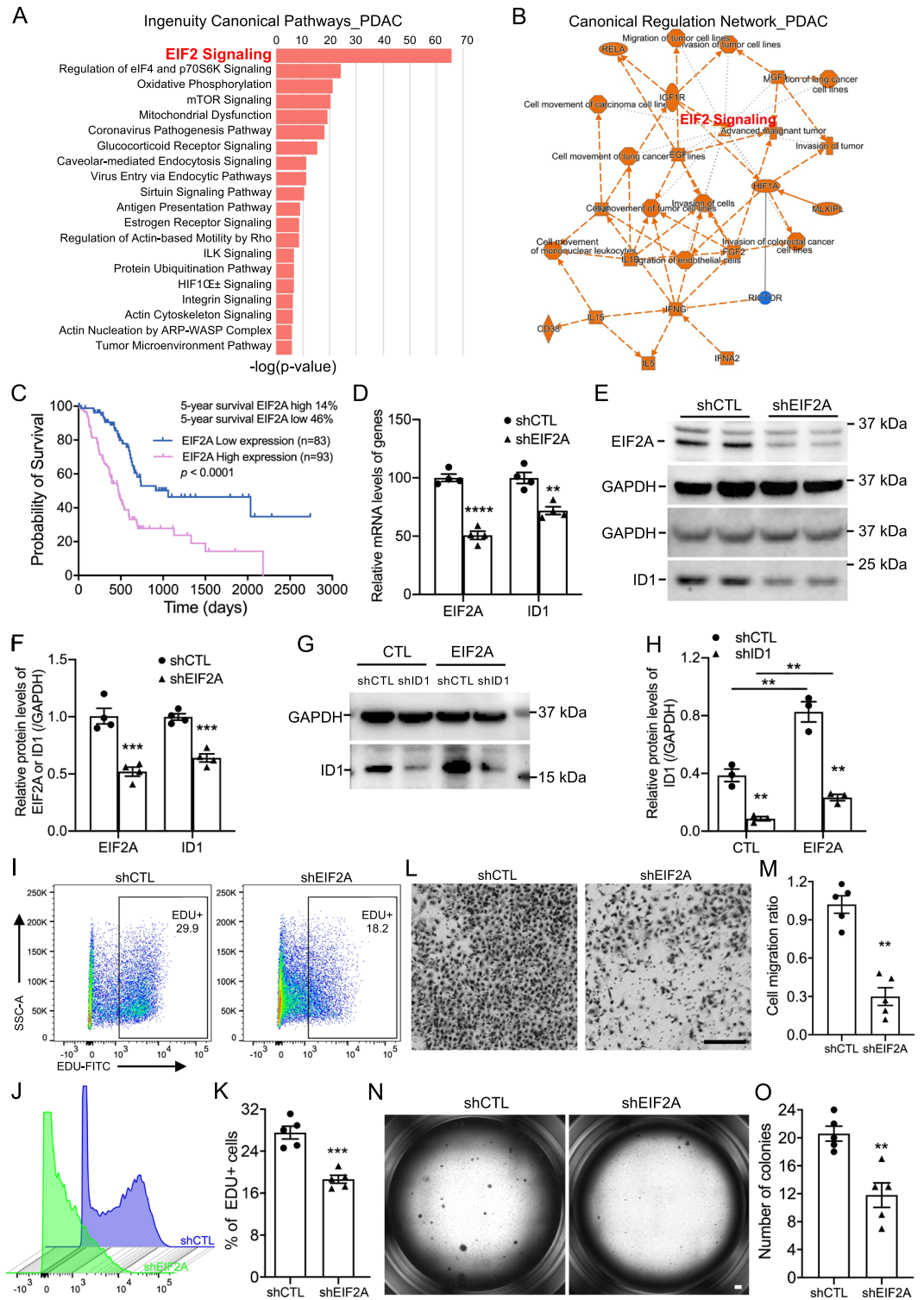


Figure 9. Blocking EIF2A signaling blunts tumorigenesis in vitro. (A,B) Top 20 ingenuity canonical pathways (A) and canonical regulation network (B) on the DE genes of PDAC cancer cells. (C) Survival probability of PDAC patients with different EIF2A expression in TCGA dataset. (D) Relative mRNA levels of *EIF2A* and *ID1* genes in HS-766T cells after *EIF2A* knockdown by qRT-PCR (n = 4). (E,F) Representative western blotting (E) and relative protein levels (F) of EIF2A and ID1 after *EIF2A* knockdown (n = 4). (G,H) Representative western blotting (G) and relative protein levels (H) of ID1 after *ID1* knockdown and recombinant EIF2A protein treatment (n = 3). (I,J) Cell proliferation of HS-766T cells after *EIF2A* knockdown by flow cytometry analysis on EDU labeled cells. (K) Quantification of the EDU+ proliferating cells after *EIF2A* knockdown in HS-766T cells (n = 5). (L,M) Cell migration (L) and the migration ratio (M) of HS-766T cells after *EIF2A* knockdown (n = 5). (N,O) Representative images of soft agar assays (N) and colony number quantification (O) of HS-766T cells after *EIF2A* knockdown (n = 5). Three independent repeats or more were performed for each experiment. Scale bar, 50 μ m. **p < 0.01; ***p < 0.001, ****p < 0.0001.

compared to normal pancreas tissues. High PERK and p-eIF2 α expression was correlated with shorter overall survival and high p-eIF2A levels and lymph node metastasis were independent prognosticators for survival of PDAC patients⁸⁰. The activation of the EIF2 signaling pathway, shown by the increased levels of key components of the EIF2 signaling pathway, p-PERK, p-eIF2A, and ATF4, significantly correlated with the knockdown of PUM1, the expression levels of which were higher in PDAC tissues than in adjacent tissues and were significantly associated with Tumor Node Metastasis (TNM) stage and overall survival time of PDAC patients⁸¹. One recent histological investigation revealed a significant down-regulation of four specific EIF subunits, namely EIF1, EIF2D, EIF3C and EIF6, suggesting not only EIF2 signaling, but also other members of the EIF family were of relevance in pancreatic tumor biology and might play a major role in translational control in PDAC⁸². In our study, EIF2 signaling pathway was the core upstream regulator of ID1 expression and PDAC development and progression. Blocking EIF2 signaling significantly reduced the expression levels of ID and attenuated the phenotypes of tumor formation related phenotypes.

To summary, our data, together with others' publications, suggested a critical role of ID1 in the development and progression of PDAC in both mouse models and human PDAC. ID1 expression marked the heterogeneity of human PDAC cancer cells and the relative expression levels were correlated with the malignance of PDAC cancer cell clusters. Targeting ID1 and the upstream regulator remarkably rescued the PDAC cell lines from tumor formation related phenotypes in vitro. These data revealed the potential of ID1 as a biomarker for PDAC diagnosis and prognosis and emphasized again the therapeutic values of ID1 in the prediction and treatment of PDAC in clinical precision medicine.

Data availability

Publicly available datasets were analyzed in the present study. The data can be found on the Gene Expression Omnibus database (GSE125588, GSE129455, GSE85241, GSE141017, GSE16515, GSE28735, GSE32676 and GSE15471) and Sequence Read Archive (PRJNA516878, PRJNA531464, PRJNA337935 and PRJNA604712). All the data used and/or generated in the current study are available from the corresponding author upon reasonable request.

Received: 28 April 2022; Accepted: 1 August 2022

Published online: 08 August 2022

References

- Kleeff, J. *et al.* Pancreatic cancer. *Nat. Rev. Dis. Primers* **2**, 16022. <https://doi.org/10.1038/nrdp.2016.22> (2016).
- Siegel, R. L., Miller, K. D. & Jemal, A. Cancer statistics, 2018. *CA Cancer J. Clin.* **68**, 7–30. <https://doi.org/10.3322/caac.21444> (2018).
- Kamisawa, T., Wood, L. D., Itoi, T. & Takaori, K. Pancreatic cancer. *Lancet* **388**, 73–85. [https://doi.org/10.1016/S0140-6736\(16\)00141-0](https://doi.org/10.1016/S0140-6736(16)00141-0) (2016).
- Siegel, R. L., Miller, K. D. & Jemal, A. Cancer statistics, 2016. *CA Cancer J. Clin.* **66**, 7–30. <https://doi.org/10.3322/caac.21332> (2016).
- Siegel, R. L., Miller, K. D., Fuchs, H. E. & Jemal, A. Cancer statistics, 2021. *CA Cancer J. Clin.* **71**, 7–33. <https://doi.org/10.3322/caac.21654> (2021).
- Zhang, Y. *et al.* Single-cell RNA sequencing in cancer research. *J. Exp. Clin. Cancer Res.* **40**, 81. <https://doi.org/10.1186/s13046-021-01874-1> (2021).
- Sun, G. *et al.* Single-cell RNA sequencing in cancer: Applications, advances, and emerging challenges. *Mol. Ther. Oncol.* **21**, 183–206. <https://doi.org/10.1016/j.omto.2021.04.001> (2021).
- Fan, J., Slowikowski, K. & Zhang, F. Single-cell transcriptomics in cancer: Computational challenges and opportunities. *Exp. Mol. Med.* **52**, 1452–1465. <https://doi.org/10.1038/s12276-020-0422-0> (2020).
- Lahnemann, D. *et al.* Eleven grand challenges in single-cell data science. *Genome Biol.* **21**, 31. <https://doi.org/10.1186/s13059-020-1926-6> (2020).
- Whattcott, C., Han, H., Posner, R. G. & Von Hoff, D. D. Tumor-stromal interactions in pancreatic cancer. *Crit. Rev. Oncog.* **18**, 135–151. <https://doi.org/10.1615/critrevoncog.v18.i1-2.80> (2013).
- Hosein, A. N. *et al.* Cellular heterogeneity during mouse pancreatic ductal adenocarcinoma progression at single-cell resolution. *JCI Insight*. <https://doi.org/10.1172/jci.insight.129212> (2019).
- Elyada, E. *et al.* Cross-species single-cell analysis of pancreatic ductal adenocarcinoma reveals antigen-presenting cancer-associated fibroblasts. *Cancer Discov.* **9**, 1102–1123. <https://doi.org/10.1158/2159-8290.CD-19-0094> (2019).
- Muraro, M. J. *et al.* A single-cell transcriptome atlas of the human pancreas. *Cell Syst.* **3**, 385–394. <https://doi.org/10.1016/j.cels.2016.09.002> (2016).
- Schlesinger, Y. *et al.* Single-cell transcriptomes of pancreatic preinvasive lesions and cancer reveal acinar metaplastic cells' heterogeneity. *Nat. Commun.* **11**, 4516. <https://doi.org/10.1038/s41467-020-18207-z> (2020).
- Yao, L. *et al.* The roles of ID-1 in human pancreatic ductal adenocarcinoma and the therapeutic effects of 2-methoxyestradiol. *Carcinogenesis* **39**, 728–737. <https://doi.org/10.1093/carcin/bgy035> (2018).
- Georgiadou, D. *et al.* VEGF and Id-1 in pancreatic adenocarcinoma: Prognostic significance and impact on angiogenesis. *Eur. J. Surg. Oncol.* **40**, 1331–1337. <https://doi.org/10.1016/j.ejso.2014.01.004> (2014).
- Huang, Y. H. *et al.* ID1 mediates escape from TGF β tumor suppression in pancreatic cancer. *Cancer Discov.* **10**, 142–157. <https://doi.org/10.1158/2159-8290.CD-19-0529> (2020).
- Bulle, A. & Lim, K. H. Beyond just a tight fortress: Contribution of stroma to epithelial-mesenchymal transition in pancreatic cancer. *Signal Transduct Target Ther.* **5**, 249. <https://doi.org/10.1038/s41392-020-00341-1> (2020).
- Nemetski, S. M. & Gardner, L. B. Hypoxic regulation of Id-1 and activation of the unfolded protein response are aberrant in neuroblastoma. *J. Biol. Chem.* **282**, 240–248. <https://doi.org/10.1074/jbc.M607275200> (2007).
- Furtunescu, F. *et al.* Breast cancer mortality gaps in Romanian women compared to the EU after 10 years of accession: Is breast cancer screening a priority for action in Romania? (review of the statistics). *Exp. Ther. Med.* **21**, 268. <https://doi.org/10.3892/etm.2021.9699> (2021).
- Aguirre, A. J. *et al.* Activated Kras and Ink4a/Arf deficiency cooperate to produce metastatic pancreatic ductal adenocarcinoma. *Genes Dev.* **17**, 3112–3126. <https://doi.org/10.1101/gad.1158703> (2003).
- DeCant, B. T., Principe, D. R., Guerra, C., di Magliano, M. P. & Grippo, P. J. Utilizing past and present mouse systems to engineer more relevant pancreatic cancer models. *Front. Physiol.* **5**, 464. <https://doi.org/10.3389/fphys.2014.00464> (2014).

23. Hingorani, S. R. *et al.* Trp53R172H and KrasG12D cooperate to promote chromosomal instability and widely metastatic pancreatic ductal adenocarcinoma in mice. *Cancer Cell* **7**, 469–483. <https://doi.org/10.1016/j.ccr.2005.04.023> (2005).
24. Stratford, J. K. *et al.* A six-gene signature predicts survival of patients with localized pancreatic ductal adenocarcinoma. *PLoS Med.* **7**, e1000307. <https://doi.org/10.1371/journal.pmed.1000307> (2010).
25. Shin, S. *et al.* Activator protein-1 has an essential role in pancreatic cancer cells and is regulated by a novel Akt-mediated mechanism. *Mol. Cancer Res.* **7**, 745–754. <https://doi.org/10.1158/1541-7786.MCR-08-0462> (2009).
26. Xu, X. *et al.* miR-30d suppresses proliferation and invasiveness of pancreatic cancer by targeting the SOX4/PI3K-AKT axis and predicts poor outcome. *Cell Death Dis.* **12**, 350. <https://doi.org/10.1038/s41419-021-03576-0> (2021).
27. Huang, H. Y. *et al.* SOX4 transcriptionally regulates multiple SEMA3/plexin family members and promotes tumor growth in pancreatic cancer. *PLoS ONE* **7**, e48637. <https://doi.org/10.1371/journal.pone.0048637> (2012).
28. He, P., Yang, J. W., Yang, V. W. & Bialkowska, A. B. Kruppel-like factor 5, increased in pancreatic ductal adenocarcinoma, promotes proliferation, acinar-to-ductal metaplasia, pancreatic intraepithelial neoplasia, and tumor growth in mice. *Gastroenterology* **154**, 1494–1508. <https://doi.org/10.1053/j.gastro.2017.12.005> (2018).
29. Diaferia, G. R. *et al.* Dissection of transcriptional and cis-regulatory control of differentiation in human pancreatic cancer. *EMBO J.* **35**, 595–617. <https://doi.org/10.15252/embj.201592404> (2016).
30. Zammarchi, F. *et al.* KLF4 is a novel candidate tumor suppressor gene in pancreatic ductal carcinoma. *Am. J. Pathol.* **178**, 361–372. <https://doi.org/10.1016/j.ajpath.2010.11.021> (2011).
31. Hartel, M. *et al.* Increased alternative splicing of the KLF6 tumour suppressor gene correlates with prognosis and tumour grade in patients with pancreatic cancer. *Eur. J. Cancer* **44**, 1895–1903. <https://doi.org/10.1016/j.ejca.2008.06.030> (2008).
32. Wang, L., Mao, Q., Zhou, S. & Ji, X. Hypermethylated KLF9 is an independent prognostic factor for favorable outcome in breast cancer. *Oncotargets Ther.* **12**, 9915–9926. <https://doi.org/10.2147/OTT.S226121> (2019).
33. Ji, P. *et al.* Kruppel-like factor 9 suppressed tumorigenicity of the pancreatic ductal adenocarcinoma by negatively regulating frizzled-5. *Biochem. Biophys. Res. Commun.* **499**, 815–821. <https://doi.org/10.1016/j.bbrc.2018.03.229> (2018).
34. Pistoni, L. *et al.* Associations between pancreatic expression quantitative traits and risk of pancreatic ductal adenocarcinoma. *Carcinogenesis*. <https://doi.org/10.1093/carcin/bgab057> (2021).
35. Liu, J. H., Chen, G., Dang, Y. W., Li, C. J. & Luo, D. Z. Expression and prognostic significance of lncRNA MALAT1 in pancreatic cancer tissues. *Asian Pac. J. Cancer Prev.* **15**, 2971–2977. <https://doi.org/10.7314/apjcp.2014.15.7.2971> (2014).
36. Li, L. *et al.* Long noncoding RNA MALAT1 promotes aggressive pancreatic cancer proliferation and metastasis via the stimulation of autophagy. *Mol. Cancer Ther.* **15**, 2232–2243. <https://doi.org/10.1158/1535-7163.MCT-16-0008> (2016).
37. Liu, P. *et al.* The lncRNA MALAT1 acts as a competing endogenous RNA to regulate KRAS expression by sponging miR-217 in pancreatic ductal adenocarcinoma. *Sci. Rep.* **7**, 5186. <https://doi.org/10.1038/s41598-017-05274-4> (2017).
38. He, Y. *et al.* Potential applications of MEG3 in cancer diagnosis and prognosis. *Oncotarget* **8**, 73282–73295. <https://doi.org/10.18632/oncotarget.19931> (2017).
39. Ma, L. *et al.* Long non-coding RNA MEG3 functions as a tumour suppressor and has prognostic predictive value in human pancreatic cancer. *Oncol. Rep.* **39**, 1132–1140. <https://doi.org/10.3892/or.2018.6178> (2018).
40. Pan, H. *et al.* A cancer cell cluster marked by lincRNA MEG3 leads pancreatic ductal adenocarcinoma metastasis. *Front. Oncol.* **11**, 656564. <https://doi.org/10.3389/fonc.2021.656564> (2021).
41. Han, T. *et al.* Coordinated silencing of the Sp1-mediated long noncoding RNA MEG3 by EZH2 and HDAC3 as a prognostic factor in pancreatic ductal adenocarcinoma. *Cancer Biol. Med.* **17**, 953–969. <https://doi.org/10.20892/j.issn.2095-3941.2019.0427> (2020).
42. Wang, J. *et al.* Prox1 activity controls pancreas morphogenesis and participates in the production of “secondary transition” pancreatic endocrine cells. *Dev. Biol.* **286**, 182–194. <https://doi.org/10.1016/j.ydbio.2005.07.021> (2005).
43. Zhang, Y. *et al.* The zinc finger protein ZBTB20 regulates transcription of fructose-1,6-bisphosphatase 1 and beta cell function in mice. *Gastroenterology* **142**, 1571–1580. <https://doi.org/10.1053/j.gastro.2012.02.043> (2012).
44. Westmoreland, J. J. *et al.* Dynamic distribution of claudin proteins in pancreatic epithelia undergoing morphogenesis or neoplastic transformation. *Dev. Dyn.* **241**, 583–594. <https://doi.org/10.1002/dvdy.23740> (2012).
45. de Oliveira, C. *et al.* Pancreatic triglyceride lipase mediates lipotoxic systemic inflammation. *J. Clin. Investig.* **130**, 1931–1947. <https://doi.org/10.1172/JCI132767> (2020).
46. Lemaire, L. A. *et al.* Bicaudal C1 promotes pancreatic NEUROG3+ endocrine progenitor differentiation and ductal morphogenesis. *Development* **142**, 858–870. <https://doi.org/10.1242/dev.114611> (2015).
47. Kraus, M. R. *et al.* Two mutations in human BICC1 resulting in Wnt pathway hyperactivity associated with cystic renal dysplasia. *Hum. Mutat.* **33**, 86–90. <https://doi.org/10.1002/humu.21610> (2012).
48. Rasanen, K., Ikonen, O., Koistinen, H. & Stenman, U. H. Emerging roles of SPINK1 in cancer. *Clin. Chem.* **62**, 449–457. <https://doi.org/10.1373/clinchem.2015.241513> (2016).
49. Wang, Y. D., Chen, W. D., Moore, D. D. & Huang, W. FXR: A metabolic regulator and cell protector. *Cell Res.* **18**, 1087–1095. <https://doi.org/10.1038/cr.2008.289> (2008).
50. Dufer, M., Horth, K., Krippeit-Drews, P. & Drews, G. The significance of the nuclear farnesoid X receptor (FXR) in beta cell function. *Islets* **4**, 333–338. <https://doi.org/10.4161/isl.22383> (2012).
51. Bertrand, C., Valet, P. & Castan-Laurell, I. Apelin and energy metabolism. *Front. Physiol.* **6**, 115. <https://doi.org/10.3389/fphys.2015.00115> (2015).
52. Strutt, B. *et al.* Ontology of the apelinergic system in mouse pancreas during pregnancy and relationship with beta-cell mass. *Sci. Rep.* **11**, 15475. <https://doi.org/10.1038/s41598-021-94725-0> (2021).
53. Brun, P. J., Wongsiriroj, N. & Blaner, W. S. Retinoids in the pancreas. *Hepatobiliary Surg. Nutr.* **5**, 1–14. <https://doi.org/10.3978/j.issn.2304-3881.2015.09.03> (2016).
54. Arregi, I. *et al.* Retinol dehydrogenase-10 regulates pancreas organogenesis and endocrine cell differentiation via paracrine retinoic acid signaling. *Endocrinology* **157**, 4615–4631. <https://doi.org/10.1210/en.2016-1745> (2016).
55. Bradford, J. A. & Clarke, S. T. Dual-pulse labeling using 5-ethynyl-2'-deoxyuridine (EdU) and 5-bromo-2'-deoxyuridine (BrdU) in flow cytometry. *Curr. Protoc. Cytom.* <https://doi.org/10.1002/0471142956.cy0738s55> (2011).
56. Paul, C. D., Mistriotis, P. & Konstantopoulos, K. Cancer cell motility: Lessons from migration in confined spaces. *Nat. Rev. Cancer* **17**, 131–140. <https://doi.org/10.1038/nrc.2016.123> (2017).
57. Borowicz, S. *et al.* The soft agar colony formation assay. *J. Vis. Exp.* <https://doi.org/10.3791/51998> (2014).
58. Hidalgo, M. *et al.* Addressing the challenges of pancreatic cancer: Future directions for improving outcomes. *Pancreatology* **15**, 8–18. <https://doi.org/10.1016/j.pan.2014.10.001> (2015).
59. Orth, M. *et al.* Pancreatic ductal adenocarcinoma: Biological hallmarks, current status, and future perspectives of combined modality treatment approaches. *Radiat. Oncol.* **14**, 141. <https://doi.org/10.1186/s13014-019-1345-6> (2019).
60. Adamska, A., Domenichini, A. & Falasca, M. Pancreatic ductal adenocarcinoma: Current and evolving therapies. *Int. J. Mol. Sci.* <https://doi.org/10.3390/ijms18071338> (2017).
61. Gharibi, A., Adamian, Y. & Kelber, J. A. Cellular and molecular aspects of pancreatic cancer. *Acta Histochem.* **118**, 305–316. <https://doi.org/10.1016/j.acthis.2016.01.009> (2016).
62. Falasca, M., Kim, M. & Casari, I. Pancreatic cancer: Current research and future directions. *Biochim. Biophys. Acta* **1865**, 123. <https://doi.org/10.1016/j.bbcan.2016.01.001> (2016).

63. Kunovsky, L. *et al.* The use of biomarkers in early diagnostics of pancreatic cancer. *Can. J. Gastroenterol.* <https://doi.org/10.1155/2018/5389820> (2018).
64. Herreros-Villanueva, M. & Bujanda, L. Non-invasive biomarkers in pancreatic cancer diagnosis: What we need versus what we have. *Ann. Transl. Med.* **4**, 134. <https://doi.org/10.21037/atm.2016.03.44> (2016).
65. Lister, J., Forrester, W. C. & Baron, M. H. Inhibition of an erythroid differentiation switch by the helix-loop-helix protein Id1. *J. Biol. Chem.* **270**, 17939–17946. <https://doi.org/10.1074/jbc.270.30.17939> (1995).
66. Ling, M. T. *et al.* Id-1 expression promotes cell survival through activation of NF-kappaB signalling pathway in prostate cancer cells. *Oncogene* **22**, 4498–4508. <https://doi.org/10.1038/sj.onc.1206693> (2003).
67. Wong, Y. C., Wang, X. & Ling, M. T. Id-1 expression and cell survival. *Apoptosis* **9**, 279–289. <https://doi.org/10.1023/b:appt.0000025804.25396.79> (2004).
68. Zhao, Z., Bo, Z., Gong, W. & Guo, Y. Inhibitor of differentiation 1 (Id1) in cancer and cancer therapy. *Int. J. Med. Sci.* **17**, 995–1005. <https://doi.org/10.7150/ijms.42805> (2020).
69. Lee, K. T. *et al.* Overexpression of Id-1 is significantly associated with tumour angiogenesis in human pancreas cancers. *Br. J. Cancer* **90**, 1198–1203. <https://doi.org/10.1038/sj.bjc.6601684> (2004).
70. Lim, Y. J. *et al.* Prognostic value of VEGF in human pancreatic ductal adenocarcinoma. *Korean J. Intern. Med.* **19**, 10–14. <https://doi.org/10.3904/kjim.2004.19.1.10> (2004).
71. Huang, C. *et al.* The expression and clinical significance of pSTAT3, VEGF and VEGF-C in pancreatic adenocarcinoma. *Neoplasma* **59**, 52–61. https://doi.org/10.4149/neo_2012_007 (2012).
72. David, C. J. & Massague, J. Contextual determinants of TGFbeta action in development, immunity and cancer. *Nat. Rev. Mol. Cell Biol.* **19**, 419–435. <https://doi.org/10.1038/s41580-018-0007-0> (2018).
73. Guasch, G. *et al.* Loss of TGFbeta signaling destabilizes homeostasis and promotes squamous cell carcinomas in stratified epithelia. *Cancer Cell* **12**, 313–327. <https://doi.org/10.1016/j.ccr.2007.08.020> (2007).
74. David, C. J. *et al.* TGF-beta tumor suppression through a lethal EMT. *Cell* **164**, 1015–1030. <https://doi.org/10.1016/j.cell.2016.01.009> (2016).
75. Lasorella, A., Benezra, R. & Iavarone, A. The ID proteins: Master regulators of cancer stem cells and tumour aggressiveness. *Nat. Rev. Cancer* **14**, 77–91. <https://doi.org/10.1038/nrc3638> (2014).
76. Kondo, M. *et al.* A role for Id in the regulation of TGF-beta-induced epithelial-mesenchymal transdifferentiation. *Cell Death Differ.* **11**, 1092–1101. <https://doi.org/10.1038/sj.cdd.4401467> (2004).
77. Hu, H. *et al.* A novel role of Id-1 in regulation of epithelial-to-mesenchymal transition in bladder cancer. *Urol. Oncol.* **31**, 1242–1253. <https://doi.org/10.1016/j.urolonc.2011.12.003> (2013).
78. Brabletz, T., Kalluri, R., Nieto, M. A. & Weinberg, R. A. EMT in cancer. *Nat. Rev. Cancer* **18**, 128–134. <https://doi.org/10.1038/nrc.2017.118> (2018).
79. Hao, P. Q. *et al.* Eukaryotic translation initiation factors as promising targets in cancer therapy. *Cell Commun. Signal* **18**, 9. <https://doi.org/10.1186/s12964-020-00607-9> (2020).
80. Wang, E. M. *et al.* Expression and clinical significance of protein kinase RNA-like endoplasmic reticulum kinase and phosphorylated eukaryotic initiation factor 2alpha in pancreatic ductal adenocarcinoma. *Pancreas* **48**, 323–328. <https://doi.org/10.1097/MPA.0000000000001248> (2019).
81. Dai, H. *et al.* PUM1 knockdown prevents tumor progression by activating the PERK/eIF2/ATF4 signaling pathway in pancreatic adenocarcinoma cells. *Cell Death Dis.* **10**, 595. <https://doi.org/10.1038/s41419-019-1839-z> (2019).
82. Golob-Schwarzl, N. *et al.* New pancreatic cancer biomarkers eIF1, eIF2D, eIF3C and eIF6 play a major role in translational control in ductal adenocarcinoma. *Anticancer Res.* **40**, 3109–3118. <https://doi.org/10.21873/anticancer.14292> (2020).

Author contributions

Y.T., Q.F.: Conception and design; Y.T., C.W.: Development of methodology; Y.T., Q.F.: Acquisition of data; Y.T., S.Z., J.L.: Analysis and interpretation of data; Y.T., C.W., Q.F.: Writing, review, and/or revision of the manuscript; C.W., Q.F.: Administrative, technical, or material support; Q.F.: Study supervision. All authors reviewed the manuscript.

Funding

This work was supported by the Scientific Research of Liaoning Provincial Education Department (Grant No. LJKZ0768) and the Young and Middle-Aged Scientific and Technological Talents Support Program of Shenyang City (Grant No. RC210042).

Competing interests

The authors declare no competing interests.

Additional information

Supplementary Information The online version contains supplementary material available at <https://doi.org/10.1038/s41598-022-17827-3>.

Correspondence and requests for materials should be addressed to Q.F.

Reprints and permissions information is available at www.nature.com/reprints.

Publisher's note Springer Nature remains neutral with regard to jurisdictional claims in published maps and institutional affiliations.



Open Access This article is licensed under a Creative Commons Attribution 4.0 International License, which permits use, sharing, adaptation, distribution and reproduction in any medium or format, as long as you give appropriate credit to the original author(s) and the source, provide a link to the Creative Commons licence, and indicate if changes were made. The images or other third party material in this article are included in the article's Creative Commons licence, unless indicated otherwise in a credit line to the material. If material is not included in the article's Creative Commons licence and your intended use is not permitted by statutory regulation or exceeds the permitted use, you will need to obtain permission directly from the copyright holder. To view a copy of this licence, visit <http://creativecommons.org/licenses/by/4.0/>.

© The Author(s) 2022